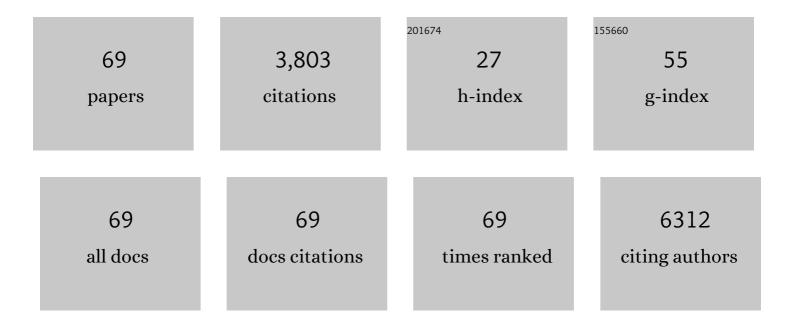
List of Publications by Year in descending order

Source: https://exaly.com/author-pdf/3724906/publications.pdf Version: 2024-02-01



WENDEL CAO

#	Article	IF	CITATIONS
1	Intercorrelated In-Plane and Out-of-Plane Ferroelectricity in Ultrathin Two-Dimensional Layered Semiconductor In ₂ Se ₃ . Nano Letters, 2018, 18, 1253-1258.	9.1	509
2	Freestanding crystalline oxide perovskites down to the monolayer limit. Nature, 2019, 570, 87-90.	27.8	398
3	Tunable intrinsic strain in two-dimensional transition metal electrocatalysts. Science, 2019, 363, 870-874.	12.6	384
4	Surface-Engineered PtNi-O Nanostructure with Record-High Performance for Electrocatalytic Hydrogen Evolution Reaction. Journal of the American Chemical Society, 2018, 140, 9046-9050.	13.7	379
5	2D metal–organic framework for stable perovskite solar cells with minimized lead leakage. Nature Nanotechnology, 2020, 15, 934-940.	31.5	258
6	Interfaces in Heterogeneous Catalysts: Advancing Mechanistic Understanding through Atomic-Scale Measurements. Accounts of Chemical Research, 2017, 50, 787-795.	15.6	128
7	Real-space charge-density imaging with sub-ångström resolution by four-dimensional electron microscopy. Nature, 2019, 575, 480-484.	27.8	127
8	Growth of Au on Pt Icosahedral Nanoparticles Revealed by Low-Dose In Situ TEM. Nano Letters, 2015, 15, 2711-2715.	9.1	106
9	Platinumâ€Based Nanowires as Active Catalysts toward Oxygen Reduction Reaction: In Situ Observation of Surfaceâ€Diffusionâ€Assisted, Solidâ€State Oriented Attachment. Advanced Materials, 2017, 29, 1703460.	21.0	102
10	Nanoscale kinetics of asymmetrical corrosion in core-shell nanoparticles. Nature Communications, 2018, 9, 1011.	12.8	87
11	Dissolution Kinetics of Oxidative Etching of Cubic and Icosahedral Platinum Nanoparticles Revealed by <i>in Situ</i> Liquid Transmission Electron Microscopy. ACS Nano, 2017, 11, 1696-1703.	14.6	84
12	Neighboring Pt Atom Sites in an Ultrathin FePt Nanosheet for the Efficient and Highly CO-Tolerant Oxygen Reduction Reaction. Nano Letters, 2018, 18, 5905-5912.	9.1	84
13	An Ionâ€Exchange Promoted Phase Transition in a Liâ€Excess Layered Cathode Material for Highâ€Performance Lithium Ion Batteries. Advanced Energy Materials, 2015, 5, 1401937.	19.5	82
14	Differential Surface Elemental Distribution Leads to Significantly Enhanced Stability of PtNi-Based ORR Catalysts. Matter, 2019, 1, 1567-1580.	10.0	82
15	Lattice and strain analysis of atomic resolution Z-contrast images based on template matching. Ultramicroscopy, 2014, 136, 50-60.	1.9	80
16	Core–Shell Nanostructured Cobalt–Platinum Electrocatalysts with Enhanced Durability. ACS Catalysis, 2018, 8, 35-42.	11.2	72
17	Revealing Surface Elemental Composition and Dynamic Processes Involved in Facet-Dependent Oxidation of Pt ₃ Co Nanoparticles via <i>in Situ</i> Transmission Electron Microscopy. Nano Letters, 2017, 17, 4683-4688.	9.1	71
18	Tailoring a Three-Phase Microenvironment for High-Performance Oxygen Reduction Reaction in Proton Exchange Membrane Fuel Cells. Matter, 2020, 3, 1774-1790.	10.0	71

#	Article	IF	CITATIONS
19	Sub-10-nm graphene nanoribbons with atomically smooth edges from squashed carbon nanotubes. Nature Electronics, 2021, 4, 653-663.	26.0	61
20	Strong electrostatic adsorption approach to the synthesis of sub-three nanometer intermetallic platinum–cobalt oxygen reduction catalysts. Nano Energy, 2021, 79, 105465.	16.0	59
21	Strong Electronic Interaction of Amorphous Fe ₂ O ₃ Nanosheets with Singleâ€Atom Pt toward Enhanced Carbon Monoxide Oxidation. Advanced Functional Materials, 2019, 29, 1904278.	14.9	51
22	Strain-Induced Corrosion Kinetics at Nanoscale Are Revealed in Liquid: Enabling Control of Corrosion Dynamics of Electrocatalysis. CheM, 2020, 6, 2257-2271.	11.7	48
23	Deterministic, Reversible, and Nonvolatile Low-Voltage Writing of Magnetic Domains in Epitaxial BaTiO ₃ /Fe ₃ O ₄ Heterostructure. ACS Nano, 2018, 12, 9558-9567.	14.6	43
24	Direct in Situ Observation and Analysis of the Formation of Palladium Nanocrystals with High-Index Facets. Nano Letters, 2018, 18, 7004-7013.	9.1	42
25	Large Negative-Thermal-Quenching Effect in Phonon-Induced Light Emissions in Mn ⁴⁺ -Activated Fluoride Phosphor for Warm-White Light-Emitting Diodes. ACS Omega, 2018, 3, 13704-13710.	3.5	41
26	Probing the dynamics of nanoparticle formation from a precursor at atomic resolution. Science Advances, 2019, 5, eaau9590.	10.3	40
27	Direct observation of elemental fluctuation and oxygen octahedral distortion-dependent charge distribution in high entropy oxides. Nature Communications, 2022, 13, 2358.	12.8	35
28	Direct Observation of Interfacial Au Atoms on TiO ₂ in Three Dimensions. Nano Letters, 2015, 15, 2548-2554.	9.1	26
29	Tuning Fe concentration in epitaxial gallium ferrite thin films for room temperature multiferroic properties. Acta Materialia, 2018, 145, 488-495.	7.9	26
30	Transmission electron microscopy with atomic resolution under atmospheric pressures. MRS Communications, 2017, 7, 798-812.	1.8	24
31	Engineering Temperatureâ€Dependent Carrier Concentration in Bulk Composite Materials via Temperatureâ€Dependent Fermi Level Offset. Advanced Energy Materials, 2018, 8, 1701623.	19.5	21
32	Structures and electronic properties of domain walls in BiFeO3 thin films. National Science Review, 2019, 6, 669-683.	9.5	18
33	Atomistic insights into the nucleation and growth of platinum on palladium nanocrystals. Nature Communications, 2021, 12, 3215.	12.8	18
34	Fast Proton Insertion in Layered H ₂ W ₂ O ₇ via Selective Etching of an Aurivillius Phase. Advanced Energy Materials, 2021, 11, .	19.5	16
35	Interaction of nanometer-sized gold nanocrystals with rutile (110) surface steps revealed at atomic resolution. Surface Science, 2014, 625, 16-22.	1.9	15
36	Thickness and defocus dependence of inter-atomic electric fields measured by scanning diffraction. Ultramicroscopy, 2020, 208, 112850.	1.9	14

#	Article	IF	CITATIONS
37	Stretchable and Multi-Metal–Organic Framework Fabrics Via High-Yield Rapid Sorption-Vapor Synthesis and Their Application in Chemical Warfare Agent Hydrolysis. ACS Applied Materials & Interfaces, 2021, 13, 31279-31284.	8.0	13
38	Boosting phonon-induced luminescence in red fluoride phosphors <i>via</i> composition-driven structural transformations. Journal of Materials Chemistry C, 2017, 5, 12105-12111.	5.5	11
39	Crystallinity after decarboxylation of a metal–carboxylate framework: indestructible porosity for catalysis. Dalton Transactions, 2020, 49, 11902-11910.	3.3	10
40	Imaging Shape-Dependent Corrosion Behavior of Pt Nanoparticles over Extended Time Using a Liquid Flow Cell and TEM. Microscopy and Microanalysis, 2014, 20, 1508-1509.	0.4	9
41	Dynamics of Transformation from Platinum Icosahedral Nanoparticles to Larger FCC Crystal at Millisecond Time Resolution. Scientific Reports, 2017, 7, 17243.	3.3	9
42	From ion to atom to dendrite: Formation and nanomechanical behavior of electrodeposited lithium. MRS Bulletin, 2020, 45, 891-904.	3.5	9
43	In situ RHEED study of epitaxial gold nanocrystals on TiO2 (110) surfaces. Applied Surface Science, 2013, 270, 661-666.	6.1	8
44	Atomic resolution tomography reconstruction of tilt series based on a GPU accelerated hybrid input–output algorithm using polar Fourier transform. Ultramicroscopy, 2015, 149, 64-73.	1.9	6
45	AutoDisk: Automated diffraction processing and strain mapping in 4D-STEM. Ultramicroscopy, 2022, 236, 113513.	1.9	5
46	A kinetic Monte Carlo study of coarsening resistance of novel core/shell precipitates. Acta Materialia, 2014, 79, 37-46.	7.9	4
47	Self-assembling epitaxial growth of a single crystalline CoFe ₂ O ₄ nanopillar array <i>via</i> dual-target pulsed laser deposition. Journal of Materials Chemistry C, 2018, 6, 4854-4860.	5.5	4
48	Polarization fluctuation of BaTiO3 at unit cell level mapped by four-dimensional scanning transmission electron microscopy. Journal of Vacuum Science and Technology A: Vacuum, Surfaces and Films, 2022, 40, 013205.	2.1	4
49	In situ Atmospheric Transmission Electron Microscopy of Catalytic Nanomaterials. MRS Advances, 2018, 3, 2297-2303.	0.9	2
50	In Situ Observations of the Dynamics of Pd@Pt Core-Shell Nanoparticles in Electrolyte. Microscopy and Microanalysis, 2021, 27, 234-236.	0.4	2
51	Oxidation of Fe Whiskers and Surface Diffusion Observed by Environmental TEM. Microscopy and Microanalysis, 2014, 20, 1864-1865.	0.4	1
52	<i>In situ</i> Cathodoluminescence and Monitoring Electronic Structure Change Using Optical TEM Holder. Microscopy and Microanalysis, 2019, 25, 2302-2303.	0.4	1
53	In Situ Observations of Abnormal Pore Size Changes of a Zirconium Based Metal-Organic Framework Using Atomic Resolution S/TEM and EELS. Microscopy and Microanalysis, 2019, 25, 1486-1487.	0.4	1
54	Multiscale Electric Field Imaging of Vortices in PbTiO3-SrTiO3 Superlattice. Microscopy and Microanalysis, 2020, 26, 466-468.	0.4	1

#	Article	IF	CITATIONS
55	Phase transition and atomic scale dynamics in chemical reactions revealed in the solid state by electron microscopy. Microscopy and Microanalysis, 2021, 27, 2210-2211.	0.4	1
56	Measurement of Local Atomic Displacements Reveals Interaction of Au Nanocrystals with Rutile (TiO2) Surface Steps. Microscopy and Microanalysis, 2014, 20, 1072-1073.	0.4	0
57	Surface Atomic Diffusion Processes Observed at Milliseconds Time Resolution using Environmental TEM. Microscopy and Microanalysis, 2014, 20, 1590-1591.	0.4	Ο
58	Materials Processes Observed using Dynamical Environmental TEM at University of Illinois. Microscopy and Microanalysis, 2015, 21, 2323-2324.	0.4	0
59	Direct Observation of Interfacial Au atoms Using STEM Depth Sectioning. Microscopy and Microanalysis, 2015, 21, 2417-2418.	0.4	Ο
60	In Situ Observation of Pt Icosahedral Nanoparticles Transformation into FCC Single Crystal. Microscopy and Microanalysis, 2016, 22, 766-767.	0.4	0
61	Evolution of Au 25 (SR)18 Nanoclusters on Ceria Surfaces during in situ Electron Beam Irradiation. Microscopy and Microanalysis, 2016, 22, 1278-1279.	0.4	Ο
62	In situ Study of Dynamics of CuAu Alloy Nanoparticles on Oxide Supports. Microscopy and Microanalysis, 2017, 23, 954-955.	0.4	0
63	Calculation of the Electric Field Based on Average Momentum Transfer Using Pixelated Electron Detector in STEM. Microscopy and Microanalysis, 2017, 23, 2104-2105.	0.4	Ο
64	Combined In Situ and Ex Situ Study on Synthesis of Nanostructured Catalyst in Solid State. Microscopy and Microanalysis, 2018, 24, 288-289.	0.4	0
65	Transmission Electron Microscopy of Catalytic Nanomaterials at Atomic Resolution. Microscopy and Microanalysis, 2019, 25, 2054-2055.	0.4	Ο
66	Measuring Charge State at the Single-Atomic-Column-Base with Four-Dimensional Scanning Transmission Electron Microscopy. Microscopy and Microanalysis, 2019, 25, 16-17.	0.4	0
67	Charge Density Mapping via Scanning Diffraction in Scanning Transmission Electron Microscopy. Microscopy and Microanalysis, 2019, 25, 18-19.	0.4	0
68	Polarization in Ferroelectric BiFeO3 Imaged in 3D Using Four-dimensional Scanning Transmission Electron Microscopy. Microscopy and Microanalysis, 2020, 26, 1132-1134.	0.4	0
69	Characterization of nanomaterials dynamics with transmission electron microscope. , 2022, , .		0